AD NUMBER
AD852601
LIMITATION CHANGES

TO:

Approved for public release; distribution is unlimited. Document partially illegible.

FROM:

Distribution authorized to U.S. Gov't. agencies and their contractors; Critical Technology; MAY 1969. Other requests shall be referred to Air Force Armament Laboratory, ATWG, Eglin AFB, FL 32542. Document partially illegible. This document contains export-controlled technical data.

AUTHORITY
afatl ltr, 4 oct 1972

AFATL-TR-69-42

Analytic and Experimental Interior Ballistics of Closed Breech Guns

by

Otto K. Heiney, 1st Lt, USAFR

MAY 1969

D D C

MAY 2 6 1969

B

AIR FORCE ARMAMENT LABORATORY

AIR FORCE SYSTEMS COMMAND • UNITED STATES AIR FORCE

EGLIN AIR FORCE BASE, FLORIDA

ANALYTIC AND EXPERIMENTAL INTERIOR BALLISTICS

OF CLOSED BREECH GUNS

by

Otto K. Heiney, 1st Lt, USAFR

FOREWORD

This report has been generated under the interior ballistic analysis portion of Project 62405094 2560. It is an extension of a propellant actuated device interior ballistic formulism developed at the Jet Propulsion Laboratory (reference 1) at Pasadena, California, under NAS 7-100. The report was written by 1st Lt O. K. Heiney, USAFR, attached to the Air Force Armament Laboratory [AFATL (ATWG)] for an annual active duty tour. Assistance of the personnel of both AFATL (ATBA) and the Armament Development and Test Center [ADTC (ADTVF-2)] with the formulation and execution of the computer program is gratefully acknowledged.

Information in this report is embargoed under the Department of State International Traffic in Arms Regulations. This report may be released to foreign governments by departments or agencies of the U. S. Government subject to approval of the Air Force Armament Laboratory (ATWG), Eglin Air Force Base, Florida, or higher authority within the Department of the Air Force. Private individuals or firms require a Department of State export license.

This technical report is approved.

CHARLES K. ARPKE, Lt Colonel, USAF
Acting Chief, Weapons Division

ii

ABSTRACT

A closed breech incremental interior ballistic formulism is presented
along with a Fortran 4 computer program which utilizes the system.
Typical input and output data, both plotted and tabular, are included.
A unique characteristic of the system is that it avoids the inaccuracies
associated with approximate analytic propellant regression expressions
in that regression rates are determined by a tabular routine. Various
pressure gradient expressions are investigated. Correlation of the
mathematical model and computer predictions to experimental device
firings are presented. A shock-driven deflagration effect which may
be initiated during the ignition transient is described and a postulated
correlation parameter defined.

(The reverse of this page is blank.)

iii

CONTENTS

ILLUSTRATIONS AND TABLES

Figure

ILLUSTRATIONS AND TABLES (CONTINUED)

vi

NOMENCLATURE

A = Bore Area

a = Acceleration

C = Arbitrary Constant

C_v = Constant Volume Gas Specific Heat

C_w = Charge Weight

E_G = Kinetic Energy of Propellant Gas

F = Force

F_p = Impetus of Propellant

g = Acceleration Due to Gravity

m_A = Pseudo Mass of Propelled Device

m_p = Mass of Propelled Device

M = Mach Number

N_B = Propellant Burned

P_{AV} = Average Plenum Pressure

P_o = Total Pressure

P_s = Shot Base Pressure

r = Regression Rate of Propellant

R = Gas Constant

S_B = Burning Surface of Propellant

T = Gas Temperature

T_o = Isochoric Flame Temperature of Propellant

V = Shot Velocity

v_c = Initial Chamber Volume

v = Gas Velocity

X = Distance from Shot Base to X_o

X_o = Initial Shot Reference

x = Arbitrary Reference Behind Shot

β = Heat Loss Factor

γ = Specific Heat Ratio of Propellant Gas

δ = Density Distribution Factor

η = Covolume of Propellant Gases

ρ = Average Density of Gas

ρ_P = Density of Propellant

ρ_O = Breech Gas Density

ρ_S = Density of Gas at Projectile

ϕ = Pressure Gradient Factor

ω_0 = Initial Propellant Web

Δ = Burning Surface Factor

(The reverse of this page is blank.)

SECTION I

INTRODUCTION

The basic interior ballistic problem of any closed breech gun system is
to determine the energy release and corresponding pressure generated by the
burning of propellant in a variable volume. From the energy balance and the
equation of state, the pressure-time or pressure-travel as well as muzzle
velocity and piezometric efficiency of the system is established, thus pro-
viding the complete ballistic solution.

The results of the analysis, Section II, are essentially contained in
equations (9) and (26) which are in an incremental form specifically tailored
for machine computation. Program listing and typical results are presented
in Section III.

The analysis in Section II considers first the energy balance of the
system in paragraph A, Section II. In paragraph B, Section II, the kinetic
energy in the propellant gas is determined. Also investigated are various
expressions for the pressure gradient from the breech to the moving shot. In
paragraph C, Section II, the constant burning surface of single perforate
propellant is demonstrated and a tabular regression routine defined.

Section IV illustrates the comparison of the presented model to experi-
mentally measured pressure histories of device firings. The experimental
set-up is described, and a shock-driven deflagration phenomenon that was
encountered is defined.

1

SECTION II

ANALYSIS

ENERGY BALANCE

The Noble-Abel equation of state is:

$$P(V - \eta) = nRT \tag{1}$$

Where η is the "covolume" of the propellant and has the units of volume/ mass which arises due to the fact that the combustion products are not perfect gases.

The central property of the propellant is its "impetus," F_p, which is qualitatively similar to the c^* of rocket propellants.

$$F_p = RT_o \tag{2}$$

Where T_o is the isochoric flame temperature of the propellant gases and F_p has units of specific energy (ft-lb/lb).

The energy equation, following the techniques in reference 2, for the system will be

$$E_1 = E_2 + E_3 + E_4, \text{ where}$$

E_1 = energy put in system from propellant combustion
E_2 = translational energy of piston
E_3 = heat loss to walls
E_4 = kinetic energy of unburned propellant and propellant gases
A = cross section of bore
v_c = initial chamber volume
X = distance from X_o to piston base.

The instantaneous free chamber volume is a function of the initial chamber volume plus the barrel volume exposed by shot motion minus volume occupied by un- burnt propellant and combustion gases. Combining equations (1) and (2) then gives

$$P \left[(v_c + AX) - \frac{(C_w - N_b)}{\rho_p} - \eta N_b \right] = \frac{N_b F_p T}{T_o} \tag{3}$$

2

Thermal and chemical energy released by propellant will be

$$E_1 = N_b C_v (T_o - T) \tag{4}$$

Translational energy of the piston will be

$$E_2 = 1/2 \, m_p \, \bar{V}^2$$

The heat loss of the gases is proportional to the distance traveled, which (following reference 3) is roughly proportional to the square of the velocity. We can, to a good approximation, say that

$$E_3 = 1/2 \, \beta m_A \, V^2$$

Using the expression developed in paragraph B, below, for the kinetic energy contained in the accelerating gas and unburned propellant, we may write

$$E_4 = 1/2 \, \frac{C_w V^2}{g\delta}$$

We may define

$$m_A = m_p + \frac{C_w}{\delta g}$$

Then

$$E_2 + E_3 + E_4 = (1 + \beta)(1/2) m_A \, V^2 \tag{5}$$

Defining Y by equation (6)

$$(Y - 1) = \frac{R}{C_v} = F_p / C_v T_o \tag{6}$$

Then from equations (4), (5), and (6)

$$N_b F_p (1 - T/T_o) = 1/2 \, (Y - 1) \, (1 + \beta) \, m_A \, V^2 \tag{7}$$

The temperature ratio is eliminated by the introduction of the equation of state to give the fundamental ballistic equation

$$N_b F_p - (\gamma - 1)(1 + \beta)\frac{m_A}{2} V^2 = P_{AV}\left[(v_c + AX) - \frac{(C_w - N_b)}{\rho_p} - \eta N_b\right] \quad (8)$$

or as a differential form of equation (8) is more convenient for incremental computation, differentiating, and taking differential chamber volume changes due to charge regression as second order; this is

$$\frac{dP_{AV}}{dt}\left[(v_c + AX) - \frac{(C_w - N_b)}{\rho_p} - \eta N_b\right] = \frac{dN_b}{dt} F_p - (\gamma-1)(1+\beta) m_A \frac{dV}{dt}\frac{dx}{dt} - P_{AV}\Lambda\frac{dx}{dt} \quad (9)$$

Equation (9) provides the basis for the complete incremental interior ballistic solution; however, two additional functions are necessary to provide required relationship in the above formulation.

The first is projectile velocity as a function of average chamber pressure, or $V = f(P_s, t, m_p)$

This relation is determined in paragraph B below. The second expression required is a value for the surface exposed to burning as a function of web fraction burned.

$$N_t = f(P_{AV}, t)$$

which is covered in paragraph C below.

PRESSURE GRADIENT AND GAS KINETIC ENERGY

The determination of the pressure gradient in the barrel is central to the ballistic solution, as the velocity of the shot is a function of the pressure at the shot while equation (9) gives a value for P_{AV}. The density distribution in the gas is also required to give a value for the gas kinetic energy. The density and pressure variations are determined for an average temperature in the combustion chamber of T_0 and also for an average temperature of $7/10 \, T_0$. This problem was first studied by La'Grange and his approach introduces the analysis.

$$\frac{\partial \rho}{\partial t} + \frac{\partial}{\partial x}(\rho v) = 0 \quad (10)$$

4

and assuming constant density

$$\frac{\partial \rho}{\partial x} = 0$$

results in equation (10) being separable with the result.

$$\frac{1}{\rho} \frac{\partial \rho}{\partial t} = - \frac{\partial v}{\partial x} = C \qquad (11)$$

Equation (11) is integrated with the boundary conditions

BD 1. $X = X_0 = 0, \ v = 0$

BD 2. $X = X \qquad , \ v = V = \frac{dx}{dt}$

$$\int_0^v dv = C \int_0^x dx$$

$$v = Cx \qquad (12)$$

at boundary 2

$$C = \frac{1}{X} \frac{dX}{dt}$$

then

$$v = \frac{x}{X} \frac{dX}{dt} \qquad (13)$$

It is thus seen the constant density assumption of La'Grange will directly result in a linear velocity profile for the gases, equation (13). Constant density is then a sufficient condition for velocity linearity, though not necessarily a necessary condition.

The kinetic energy in the gas using the above approach is then

$$E_G = 1/2 \int_0^x A\rho v^2 \ dx = \frac{A\rho}{2} v^2 \int_0^x \frac{x^2}{X^2} \ dx = (1/2)(1/3) A\rho X V^2$$

but

$$A\rho X = \frac{C_w}{g}$$

5

then

$$E_G = (1/2) \, (1/3) \, \frac{C_w \, V^2}{g} = 1/2 \, \frac{C_w \, V^2}{\delta g} \qquad (14)$$

where

$\delta = 3$ for the La'Grange solution.

The factor δ was introduced by Hirschfelder (reference 3) in his extension of the work of Kent (reference 4) who allowed the gas density to vary and solved for δ as a function of the charge to projectile mass ratio.

Solutions of the form $\delta = f \, (C_w/m_p g)$

are useful for the approximate closed form ballistics of Hirschfelder but are of less utility for incremental computer solvable interior ballistic system discussed here. The results of La'Grange ($\delta = 3$) essentially state that the energy in the accelerating gas is equivalent to $1/3$ of the gas mass traveling at shot velocity. This is a good approximation at velocities where the gas density is almost constant. It falls apart, as would be expected, at velocities where the density is no longer uniform.

For incremental computations, δ is most effectively formulated as a function of shot velocity. To do this, it is first necessary to describe the density variation behind the projectile as a function of shot velocity. It is then assumed that a linear velocity gradient exists behind the shot and also that isentropic flow relations may be used during an interval to describe the flow behind the shot.

This requires that the flow during the short interval considered be looked upon as "quasi-isentropic." From reference 5, the density ratio is then

$$\rho/\rho_0 = (1 + \frac{\gamma - 1}{2} \, \frac{v^2}{gRT})^{1/\gamma - 1} \qquad (15)$$

The question then arises as to what temperature should be used to define the speed of sound in the environment of the burning gases. An upper bound for this temperature would be the isochoric flame temperature of the gases T_0; a reasonable lower bound would be $7/10 \, T_0$. The analysis is then conducted with the above values as bounds.

The results of equation (15) are plotted on Figure 1 for a $\gamma = 1.222$ and an $RT_0 = 375,000$ ft-lb/lb.

6
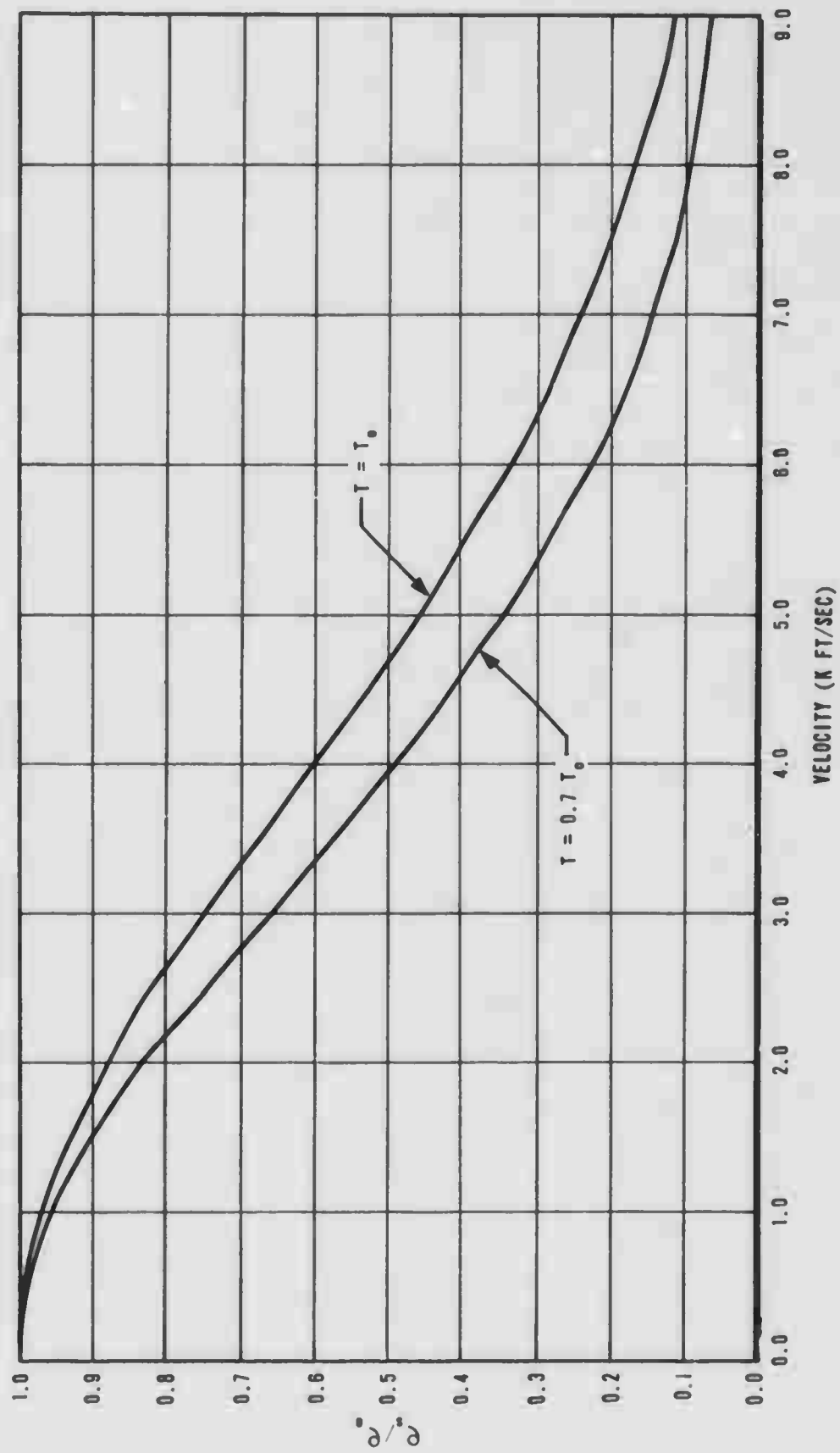
Figure 1. Density Gradient as Function of Shot Velocity.

7

The energy increment in a small control volume of gas will then be

$$E_I = 1/2 \ \rho_N \ V_N^2 \ A\Delta X_N$$

$$E_G = \frac{A\rho_0}{2} \ \sum \frac{\rho_N}{\rho_0} V_N^2 \ \Delta X_N = 1/2 \ \frac{C_w}{g\delta} \ V^2 \tag{16}$$

The value of δ, for a given velocity, is determined by performing the numerical summation of equation (16) on a digital computer. The results of this procedure are plotted on Figure 2. As would be expected at low velocities, the value of δ approaches 3.0. The results of δ as a function of velocity is then fed into the main ballistic program as data and allows for the computation of the value of the kinetic energy of the gas.

PRESSURE GRADIENT

The necessity of relating $P_s = f (P_{AV})$ has been explained above. The approach used here is to relate P_s to P_0 by two independent methods and then empirically determine a P_{AV} to P_s relationship. A value for the ratio of P_s/P_0 may be obtained by means of the "quasi-isentropic" assumption used for densities above.

$$P/P_0 = \left(1 + \frac{\gamma - 1}{2} \ \frac{v^2}{gRT} \right)^{-\gamma/\gamma-1} \tag{17}$$

The results of this relation are plotted on Figures 3 and 4 for the temperatures $T = T_0$ & $T = .7T_0$ respectively.

Another approach to the pressure gradient solution would be to assume a constant temperature process. In which case Euler's equation and the equation of state will give:

$$P = \rho RT \tag{18}$$

$$vdv = - \frac{dp}{\rho} \tag{19}$$

combining equations (18) and (19) and integrating

$$\int_0^v \ vdv = -\int_{P_0}^{P_s} \frac{RT}{P} dP$$

8
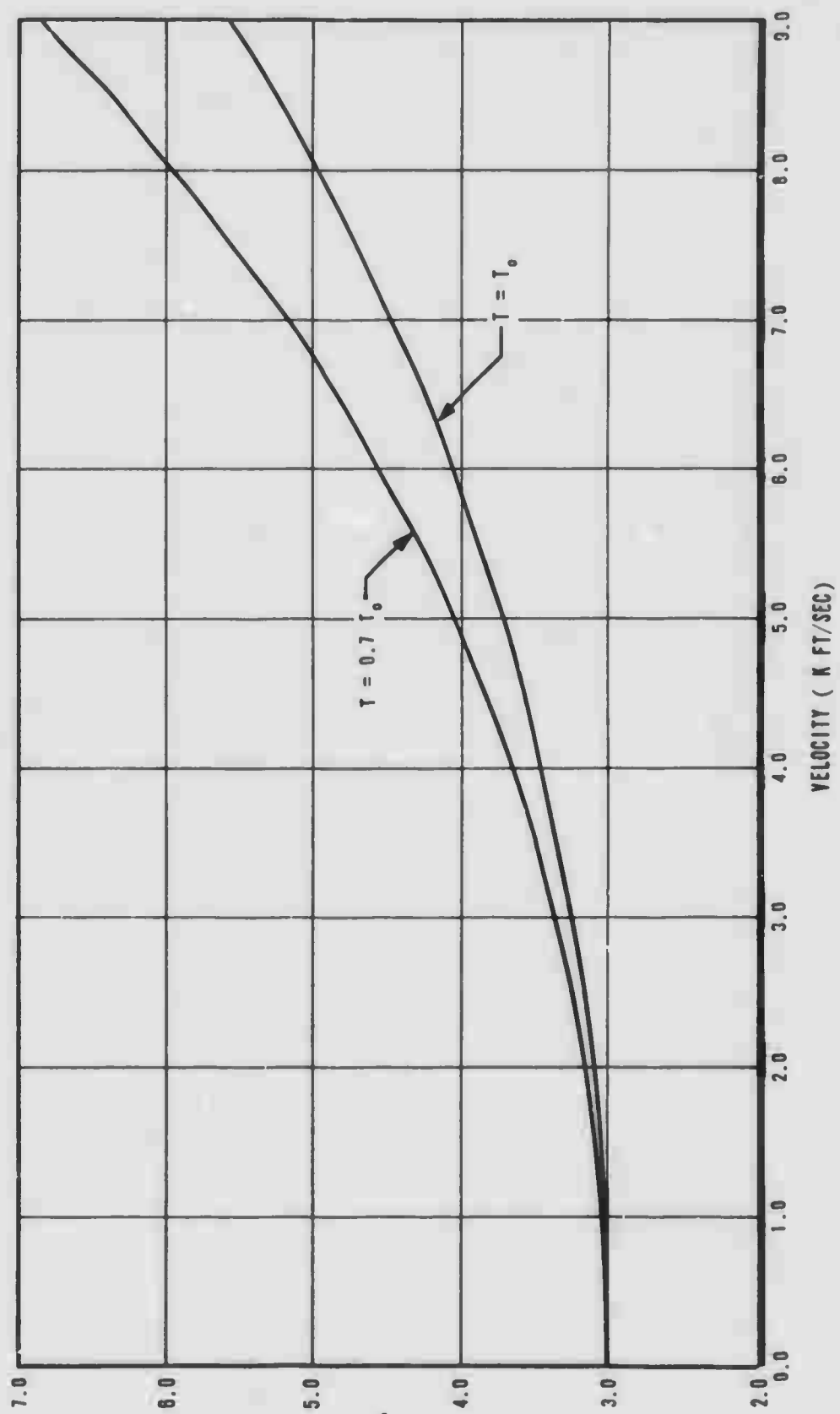
Figure 2. δ Value as Function of Projectile Velocity.

9

$$\frac{v^2}{2} = -RT \ln (P_s - P_o) \tag{20}$$

The results of equation (20) are also plotted on Figures 3 and 4. The constant temperature equation predicts a lower shot pressure than the quasi-isentropic relation. To relate P_s to P_{AV} then, a heuristically reasonable approach would be to assume that a relation of the form

$$P_s/P_{AV} = \left(1 + \frac{\gamma - 1}{2\phi} \frac{v^2}{gRT}\right)^{-\gamma/\gamma-1} \tag{21}$$

with $\phi > 1$ would be satisfactory. To investigate this possibility, it is necessary to develop a value for P_{AV} which has only the gas acceleration energy accounted for. This is done as follows:

$$P_o v_c - \frac{mv^2}{2\delta} = P_{AV} v_c$$

$$P_{AV}/P_o = 1 - \frac{v^2}{2\delta \ gF_p(T/T_o)} \tag{22}$$

Using the expression developed for $\delta = f(v)$ with $\phi = 1.5$ the combined results of equations (21) and (22) will give a value for P_s/P_o which is again plotted on Figures 3 and 4. It is seen that this value of ϕ gives consistent results for both temperature extremes. It is used in the interior ballistic formulism to relate the average pressures generated by equation (9) to the pressure at the base of the shot required for the equation of motion, as shown below.

$$V = V_o + at \tag{23}$$

$$a = \frac{P_s A}{m_p} \tag{24}$$

$$P_s = \left[1 + \frac{\gamma-1}{2\phi} M^2\right]^{-\gamma/\gamma-1} P_{AV} \tag{25}$$

then

$$V = V_o + \frac{A P_{AV}}{m_p} \left[1 + \frac{(\gamma-1)}{3} \frac{v^2}{g\gamma F_p}\right]^{-\gamma/\gamma-1} \tag{26}$$

10
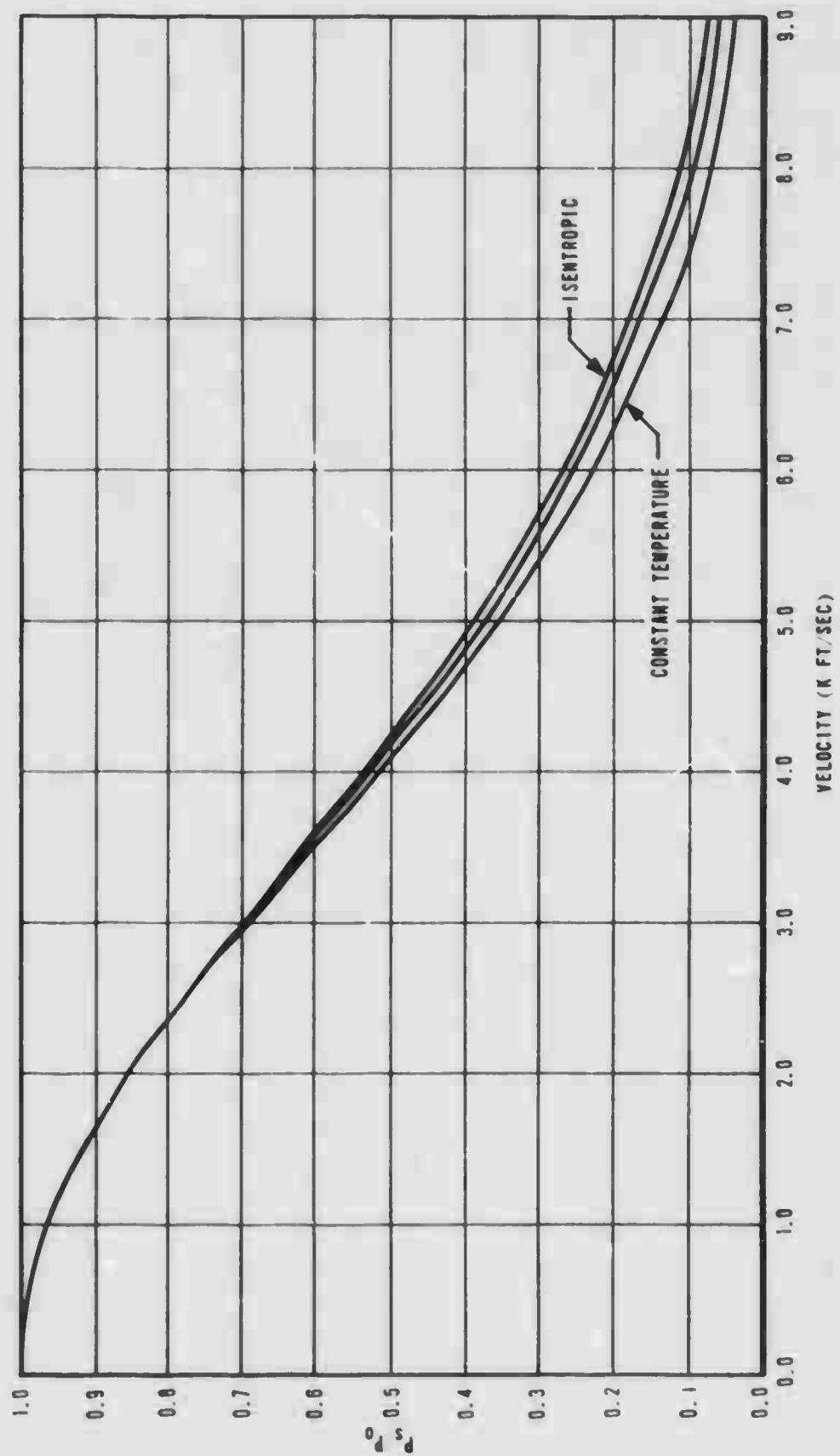
Figure 3. Shot Pressure to Static Pressure Ratio, $T = T_o$.

11
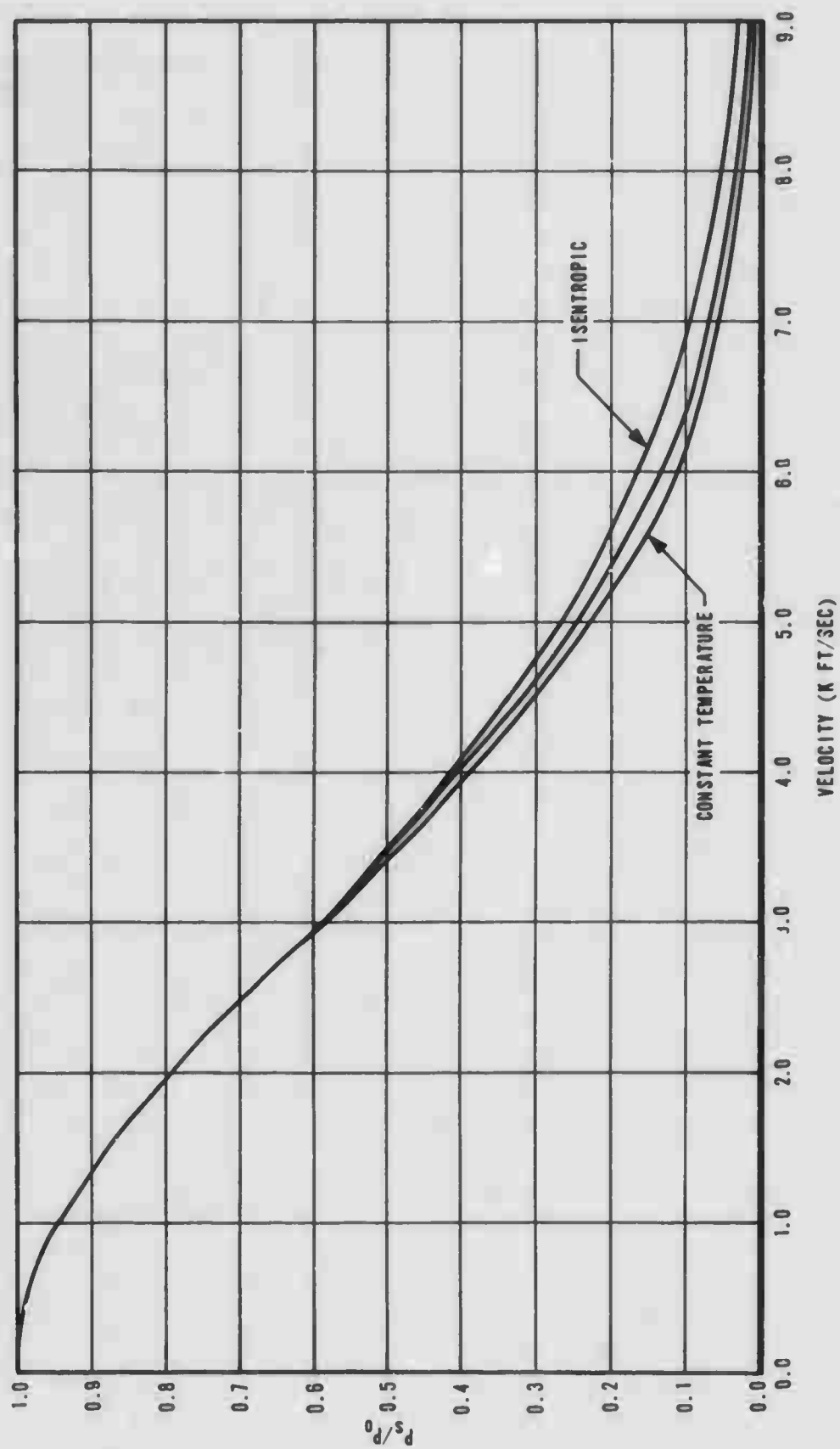
Figure 4. Shot Pressure to Static Pressure Ratio, $T = .7T_o$

12

Equation (26) thus provides the necessary relationship to solve for the projectile motion once the average chamber pressure is shown. The final information required is an expression for the total rates of combustion.

GAS PRODUCTION

The time rate of gas production is simply written as

$$\frac{dN_B}{dt} = r \, S_B \, \rho_p$$

In most prior interior ballistic formulisms the approximation $r = BP^n$ with constant N has been made. Frequently, for closed form solutions, the often questionable assumption that $N = 1$ is made. For a numeric solution, however, no approximations are required. Burning rates as a function of pressure, for currently used propellants, are tabulated in reference 7. These values are read into the program as data, and a tabular interpolation routine in the program determines the correct burning rate. Thus all recourse to Vielle's law has been avoided.

The surface of burning of single perforate propellants is very nearly constant as shown below. For other forms, such as cord, disk, and multiperforate, various empirical "form" functions exist to evaluate burning surface as a function of unburned web. These functions are covered in detail in references 3, 6, and 8.
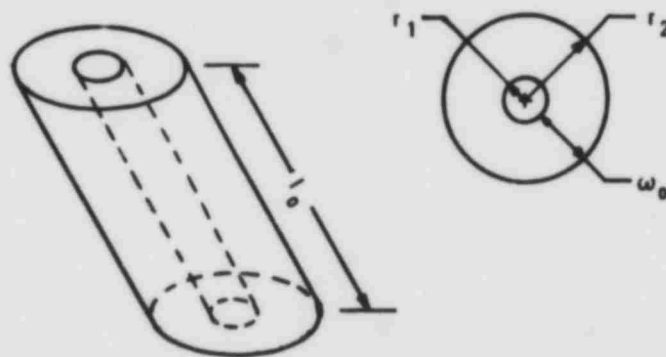
$\omega_o = r_{2,o} - r_{1,o}$ for a propellant with $\frac{\omega_o}{l_o} \ll 1$.

Burning surface for each grain will be

$$S_{I,o} = 2 l_o \, \pi \, (r_2 + r_1)$$

after a burning increment of Δr

13

$$S_{I,t} = 2 \, l_o \pi \left([r_2 - \Delta r] + [r_1 + \Delta r] \right) = 2 \, l_o \pi (r_2 + r_1)$$

thus at all times the burning surface is constant.

Volume of grain $= l_o \pi (r_2{}^2 - r_1{}^2)$

$N' =$ Number of grains/unit mass

Then the burning surface/unit mass of the propellant will be

$$\frac{S_B}{C_w} = \frac{S_I \, N'}{\rho_p V_o N'} = \frac{2 \, l_o \pi (r_2 + r_1)}{\rho_p \, l_o \pi (r_2 - r_1)(r_2 + r_1)} = \frac{2}{\rho_p \, \omega_o}$$

or

$$S_B = \frac{2}{\rho_p \, \omega_o} \, C_w \qquad\qquad (27)$$

Thus equations (9), (26), and (27) plus burning rate data provide the relationships necessary to solve for peak pressure, muzzle velocity and complete pressure-time, pressure-travel, and velocity-travel of any type of closed breech weapon.

14

SECTION III

COMPUTER PROGRAM

INPUT DATA AND USAGE

The input data for the program is in two parts. The first is the burning rate and impetus data for the propellant and may remain unchanged as long as one type of propellant is used. The second type card d lineates the exact parameters for one given case and will change for each case. Propellant data are determined from the tables in references 7 and 9.

PROPELLANT CARDS.

1st CARD

Columns	Data	Decimal Point	Units
1-8	Impetus of Propellant	7	Ft-Lb/Lb
12-16	Specific Heat Ratio of Gases	13	Dimensionless
20-24	Density of Propellant	20	$Lb/In.^2$
28-31	Covolume of Gases	30	$In.^3/Lb$
33-36	Propellant Type	Alpha Meric	

2nd AND 3rd CARDS

20 reference pressures - 10 per card from 500 to 200,000 psia.

4th AND 5th CARDS

20 burning rates taken from reference 7 at pressures listed above.

6th AND 7th CARDS

20 reference velocities taken from 0 to 12,000 ft/sec.

8th AND 9th CARDS

Density distribution factor appropriate to propellant used and corresponding to velocity listed above. Values can be extracted from Figure 2.

PROBLEM CARDS.

Columns	Data	Decimal Point	Units
1-7	Bore Area	4	In.^{2}
8-14	Chamber Volume	11	In.^{3}
15-21	Projectile Weight	19	Lb
22-28	Barrel Length	27	In.
29-35	Propellant Web	31	In.
36-42	Heat Loss	40	Dimensionless
43-49	Charge Weight	44	Lb
50-56	Shot Start Press	56	Lb/In.^{2}

As many problem cards as desired may be loaded after the data for
a given propellant and will be handled sequentially by the program.
Data in the above format is illustrated in Table I.

RESULTS

Typical output is illustrated in Figures 5 and 6 and Tables II and
III. Output includes time from propellant ignition, chamber pressure,
shot base pressure, projectile velocity, chamber pressure slope, and dis-
tance traveled for a typical 25mm. The two sample cases are identical
except for a decrease in charge weight in the latter. Subsequent to the
case run, additional computations of extrapolated muzzle velocity to the
specified barrel length, ballistic efficiency, and piezometric efficiency
are also made. Following each printed output is the pressure-travel plot
generated by the computer, which is also a standard output. It should
be noted that the program is currently set up to run single perforate
uninhibited propellant. For other forms, a proper form function, as
mentioned above, must be inserted in the program. The heat loss factor,
β, has a value of between .3 to .4 for a 25mm and will be somewhat larger
for smaller bores and less for larger bore weapons.

COMPUTER PROGRAM

The FORTRAN Program listing used is given as Table IV. Run time
on the 7094 computer is quite short (about .05 second per case). The
program number is 958, and it is being maintained by ADTC (ADTVF-2).

16

TABLE I. PROGRAM INPUT: TYPI

	1 2 3 4 5 6 7 8	9 10 11 12 13 14 15 16 17 18 19 20	21 22 23 24 25 26 27 28 29 30	
Typical Propellant Cards	3.46180.	1.252	.0603 29.69	M-1
	300.	500. 700.	1000.	15(
	6000.	8000. 10000. 20000.		3000
	.13	.2	.28 .38	.
	1.72	2.20	2.70 4.6	6.
	0.	500. 1000.	1500.	200
	5000.	5500. 6000.	6500.	700
	3.	3.	3.05 3.1	3.
	4.05	4.3	4.55 4.85	5.
Case Data Cards	.761 5.74	.397 69.	.022	
	.761 5.74	.397 69.	.022	

								61 62 63 64 65 66 67 68 69 70	71 72 73 74 75 76 77 78 79 80
M - 10									
1500.	2000.	2500..	3000.		4000.		5000.		
30000.	40000.	50000.	70000.		100000.	200000.			
.52	.68	.81	.96		1.2		1.45		
6.7	8.3	9.6	12.2		15.8		25.		
2000.	2500.	3000.	3500.		4000.		4500.		
7000.	7500.	8000.	8500.		9000.	12000.			
3.18	3.25	3.38	3.50		3.70		3.85		
5.2	5.55	5.95	6.40		7.00	12.0			
22	.3 .20	4000.							
22	.3 .18	4000.							

17

TABLE II. COMPUTER PRINTOUT OF 20MM PERFORMANCE 0.015 WEB.

SHOT WT.	CHARGE	WEB	M.LENGTH	CMB VOL	BORE AREA
.60	.200	.0220	64.0	5.74	.76

PROPELLANT USED IN DEVICE IS M-10

TIME	CHAMB PRES	TRAVEL	PROP BURNED	PRES SLOPE	VELOCITY	HS PRES
.0000	4000.0	.001	.0027	37466827.5	6.17	4000.0
.0000	4936.7	.004	.0060	44723334.8	13.78	4936.7
.0001	6054.8	.009	.0099	53923001.5	23.11	6054.7
.0001	7402.8	.018	.0146	63735680.1	34.52	7402.7
.0001	8996.2	.031	.0202	75458912.4	48.39	8995.9
.0001	10882.7	.049	.0267	87596429.3	65.17	10881.9
.0001	13072.6	.070	.0341	99010671.9	85.32	13070.9
.0002	15567.9	.099	.0427	111229256.8	109.28	15544.5
.0002	18328.4	.134	.0524	124020755.7	137.53	18322.1
.0002	21429.1	.183	.0635	137938537.0	170.55	21417.0
.0003	24877.6	.239	.0763	152968938.1	208.87	24855.9
.0003	28701.8	.309	.0909	167549065.0	253.06	28664.4
.0003	32840.5	.392	.1072	176296540.3	303.66	32827.6
.0003	37247.8	.442	.1251	179851794.3	361.01	37195.2
.0003	41744.7	.610	.1445	175555371.8	425.19	41631.6
.0004	46243.1	.748	.1652	167942188.3	496.08	45483.8
.0004	50631.7	.908	.1871	153298853.6	573.26	50061.6
.0004	54264.2	1.043	.2102	134076228.8	656.09	53733.5
.0005	57416.1	1.203	.2343	.111180355.0	743.78	56874.4
.0005	60345.6	1.540	.2592	85908750.3	835.37	59405.4
.0005	62563.3	1.805	.2847	59766233.0	929.80	61253.2
.0005	64037.4	2.098	.3107	34247727.2	1026.00	62405.8
.0006	64843.6	2.420	.3369	10637852.3	1122.95	62887.1
.0006	65179.6	2.772	.3632	-10126502.8	1219.70	62755.0
.0006	64906.4	3.152	.3894	-27508989.0	1315.42	62092.0
.0006	64271.7	3.561	.4154	-41348734.5	1409.45	60993.7
.0007	63145.0	3.997	.4411	-51783295.0	1501.27	59558.5
.0007	61490.6	4.441	.4665	-59150429.2	1590.50	57874.3
.0007	60411.6	4.951	.4914	-63879372.3	1676.89	56038.3
.0007	58814.6	5.447	.5158	-66465412.9	1760.30	54105.2
.0008	57153.0	6.007	.5397	-67365417.6	1840.68	52135.2
.0008	55468.8	6.571	.5632	-66986763.1	1918.02	50170.8
.0008	53794.2	7.157	.5861	-65674416.0	1992.40	48243.3
.0008	52152.3	7.766	.6085	-63704183.9	2063.89	46374.8
.0009	50549.6	8.345	.6305	-61315026.5	2132.62	44579.1
.0009	49026.7	9.045	.6521	-58659080.6	2198.70	42865.5
.0009	47560.7	9.714	.6732	-55868375.1	2262.24	41238.3
.0009	46143.6	10.402	.6938	-53036011.8	2323.48	39648.7
.0010	44437.7	11.108	.7141	-50228279.9	2382.44	38245.8
.0010	43542.0	11.831	.7341	-47490913.4	2439.29	36877.2
.0010	42334.9	12.571	.7538	-44854162.1	2494.16	35589.3
.0010	41773.1	13.327	.7729	-42336798.0	2547.16	34378.2
.0011	40714.6	14.099	.7918	-39942959.8	2598.40	33239.6
.0011	39216.4	14.886	.8104	-37834121.4	2647.94	32164.2
.0011	34270.4	15.694	.8286	-35874677.8	2696.03	31159.4
.0011	37373.6	16.503	.8465	-34016715.2	2742.60	30205.8
.0012	36673.1	17.333	.8641	-32251274.3	2787.77	29305.0
.0012	35716.6	18.176	.8814	-30606694.1	2831.64	28453.8
.0012	34941.8	19.032	.8985	-29049746.5	2874.26	27640.8
.0013	34226.6	19.900	.9162	-27586372.1	2915.52	26887.0

.0011		14.884	.8106	-37836121.6	2647.09	32166.2
.0011	34216.4	15.688	.8286	-35874977.8	2696.03	31159.4
.0011	37373.6	16.507	.8465	-34016718.2	2742.60	30205.8
.0012	36423.1	17.337	.8641	-32261274.3	2787.77	29305.0
.0012	35716.4	14.176	.8814	-30606694.1	2831.64	28453.8
.0012	36491.8	14.032	.8985	-29049746.5	2874.26	27648.8
.0012	36226.7	14.900	.9142	-27586377.1	2915.72	26887.0
.0013	35345.5	20.781	.9317	-26212013.9	2956.05	26165.7
.0013	32840.2	21.674	.9480	-24921858.7	2995.34	25482.1
.0013	32257.2	22.578	.9640	-23711010.3	3033.62	24833.7
.0013	31666.0	23.494	.9799	-22574981.6	3070.96	24218.2
.0014	31100.0	24.421	.9955	-21508658.8	3107.39	23567.3
.0014	30562.3	25.358	1.0109	-20507440.1	3142.97	23077.3
.0014	30049.6	26.306	1.0109	-19514044.1	3177.73	22548.0
.0014	28421.6	27.264	1.0109	-42079247.1	3210.98	21567.3
.0015	27869.5	28.233	1.0109	-39307761.8	3242.83	20658.7
.0015	28884.4	29.210	1.0109	-36781676.8	3273.38	19815.2
.0015	24967.3	30.194	1.0109	-34474815.8	3302.72	19030.6
.0015	25105.6	31.141	1.0109	-32364149.2	3330.93	18299.5
.0016	24296.1	32.195	1.0109	-30429391.5	3358.09	17617.0
.0016	23535.6	33.206	1.0109	-28652649.5	3386.26	16978.6
.0016	22919.2	34.225	1.0109	-27018116.0	3409.51	16380.7
.0017	22163.4	35.252	1.0109	-25511803.9	3433.90	15814.7
.0017	21506.0	36.245	1.0109	-24121315.8	3457.48	15292.5
.0017	20903.0	37.326	1.0109	-22835643.9	3480.29	14746.4
.0017	20332.1	38.373	1.0109	-21644997.4	3502.38	14228.9
.0018	19790.9	39.427	1.0109	-20540575.0	3523.79	13887.7
.0018	19277.6	40.488	1.0109	-19514044.1	3544.56	13470.7
.0018	14789.6	41.554	1.0109	-18559266.0	3564.72	13076.3
.0019	14325.6	42.626	1.0109	-17669837.6	3584.30	12702.7
.0019	17883.9	43.705	1.0109	-16840198.1	3603.34	12348.3
.0019	17062.4	44.784	1.0109	-16065304.5	3621.85	12011.9
.0019	17061.2	45.878	1.0109	-15340616.5	3639.88	11642.1
.0019	16477.7	46.972	1.0109	-14662039.4	3657.43	11367.9
.0020	16311.1	48.072	1.0109	-14025877.4	3674.54	11094.2
.0020	15984.5	49.177	1.0109	-13428774.7	3691.23	10621.9
.0020	15624.4	50.247	1.0109	-12867707.7	3707.50	10556.3
.0020	14160.4	51.401	1.0109	-12339921.0	3723.39	10306.6
.0021	14494.6	52.571	1.0109	-11842912.5	3738.91	10065.9
.0021	14493.5	53.645	1.0109	-11374404.7	3754.07	9635.6
.0021	14413.2	54.773	1.0109	-10932321.5	3768.90	9615.2
.0022	13874.0	55.906	1.0109	-10514767.4	3783.40	9403.9
.0022	13625.0	57.043	1.0109	-10120009.8	3797.58	9201.3
.0022	13341.3	58.144	1.0109	-9746462.7	3811.47	9006.8
.0022	13146.6	59.330	1.0109	-9392672.2	3825.06	8840.0
.0023	12920.1	60.479	1.0109	-9057306.3	3838.38	8640.5
.0023	12701.6	61.633	1.0109	-8739133.1	3851.44	8467.9
.0023	12440.7	62.790	1.0109	-8437030.6	3864.24	8301.8
.0023	12286.4	63.951	1.0109	-8149958.1	3876.79	8141.8
.0024	12090.0	65.116	1.0109	-7876957.4	3889.10	7987.7
.0024	11899.6	66.245	1.0109	-7617144.3	3901.19	7834.0
.0024	11715.3	67.457	1.0109	-7369701.3	3913.05	7695.7
.0024	11537.0	68.633	1.0109	-7133872.1	3924.70	7557.3
		69.812	1.0109	-6908956.3	3936.15	7423.6

PIEZOMETRIC PRESSURE IS 21734.75

MUZZLE VELOCITY IS 3924.3 FEET PER SECOND

PIEZOMETRIC EFFICIENCY IS 33.4 PERCENT

CORRECTED PIEZOMETRIC EFFICIENCY IS 37.9 PERCENT
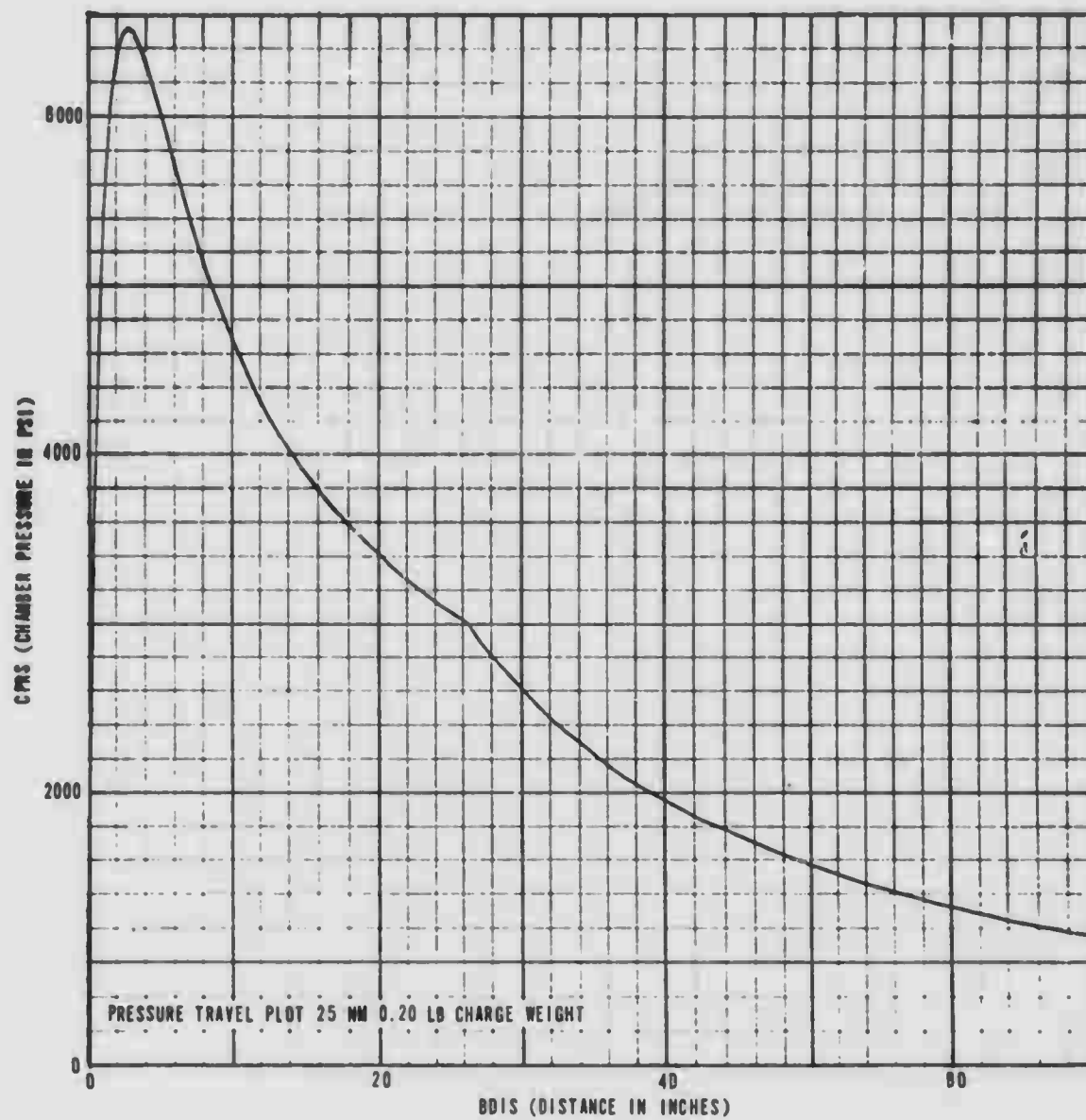
BALLISTIC EFFICIENCY IS 34.7 PERCENT

18

Figure 5. Graph of 20mm Performance 0.015 Web.

19 (The reverse of this page is blank.)

TABLE III. COMPUTER PRINTOUT OF 20MM PERFORMANCE 0.020 WEB.

SHOT WT.	CHARGE	WEB	B.LENGTH	CMB VOL	HUME AREA
.44	.140	.0220	69.0	5.74	.76

PROPELLANT USED IN DEVICE IS M-10

TIME	CHAMB PRES	TRAVEL	PROP BURNED	PRES SLOPE	VELOCITY	BS PRES
.0000	4000.0	.001	.0027	29640546.3	6.17	4000.0
.0000	4741.0	.004	.0059	34139304.6	13.48	4741.0
.0001	5546.5	.009	.0095	39557022.5	22.10	5596.5
.0001	6583.6	.017	.0138	45465753.5	32.25	6583.3
.0001	7720.1	.029	.0146	51784485.4	44.15	7719.8
.0001	9016.4	.044	.0247	59074131.1	58.05	9016.3
.0002	10691.6	.064	.0305	66498321.2	74.22	10690.6
.0002	12156.1	.089	.0376	72872565.5	92.45	12152.1
.0002	13975.9	.120	.0455	79411508.7	114.49	13972.3
.0002	15961.2	.158	.0542	85970003.4	139.09	15956.9
.0003	18110.6	.204	.0638	92360045.9	167.00	18100.0
.0003	20419.6	.260	.0745	98556620.7	198.65	20402.6
.0003	22819.6	.326	.0863	105094001.4	233.69	22856.2
.0003	25310.6	.400	.0994	110832946.5	272.95	25669.2
.0004	27841.7	.488	.1138	115404895.7	316.65	28218.7
.0004	31146.6	.590	.1294	117065760.1	364.36	31073.5
.0004	34093.6	.707	.1661	114717553.1	416.71	33945.3
.0004	36901.6	.841	.1639	110128894.4	473.40	36769.9
.0005	39714.5	.992	.1827	103277387.3	534.21	39449.3
.0005	42294.5	1.162	.2022	92745849.4	548.46	41937.1
.0005	44616.6	1.352	.2224	80477086.9	666.91	44140.6
.0005	46628.1	1.563	.2433	66976117.0	737.85	46012.5
.0006	48302.7	1.796	.2660	52837290.0	811.11	47523.3
.0006	49623.7	2.050	.2863	38621843.1	886.13	48657.3
.0006	50540.2	2.327	.3043	24854665.1	962.31	49916.8
.0006	51210.6	2.627	.3305	11479920.5	1039.11	49814.5
.0007	51510.1	2.950	.3527	333017.8	1116.00	49877.2
.0007	51518.6	3.297	.3750	-9870462.7	1192.53	49660.2
.0007	51271.7	3.666	.3972	-18524847.0	1268.29	49163.9
.0007	50800.6	4.057	.4192	-25643059.4	1342.95	48431.4
.0008	50147.3	4.471	.4411	-31284109.7	1416.25	47564.8
.0008	49345.5	4.907	.4627	-35579106.4	1487.98	46652.4
.0008	48456.6	5.366	.4690	-38684249.1	1557.98	45506.4
.0008	47526.6	5.841	.5052	-40761914.1	1626.15	46221.3
.0009	46600.6	6.330	.5260	-41986575.4	1692.44	42997.1
.0009	45660.0	6.657	.5465	-42509456.2	1756.81	41755.5
.0009	46797.2	7.397	.5660	-42478766.8	1819.27	40513.9
.0009	43335.1	7.944	.5865	-42013647.4	1879.83	39266.3
.0010	42556.6	8.521	.6060	-41218403.8	1938.54	38083.1
.0010	41256.5	9.111	.6252	-40180924.4	1995.65	36911.9
.0010	40249.2	9.713	.6442	-38970827.1	2050.60	35778.0
.0011	39275.6	10.361	.6628	-37809060.2	2104.04	34686.2
.0011	38330.6	10.940	.6810	-36602359.1	2155.93	33631.7
.0011	37415.8	11.634	.6990	-35328732.4	2206.21	32618.3
.0011	36532.3	12.303	.7166	-34019066.4	2255.00	31963.7
.0012	35681.7	12.947	.7339	-32697370.3	2302.35	30713.1
.0012	34861.6	13.646	.7509	-31342032.7	2348.32	29823.1
.0012	34072.7	14.394	.7676	-30086870.3	2392.97	28971.4
.0012	33317.5	15.159	.7800	-28822040.7	2436.40	28135.2
.0013	32567.6	15.867	.8002	-27594785.4	2478.62	27307.4
.0013	31917.1	16.607	.8181	-26410050.2	2519.69	26636.6
.0013	31256.3	17.349	.8318	-25269694.5	2559.68	25934.1
.0013	30625.2	18.143	.8472	-24175267.3	2598.63	25236.0
.0013	30020.9	18.928	.8625	-23124531.7	2636.00	24625.1

PIEZOMETRIC PRESSURE IS 19071.34

MUZZLE VELOCITY IS 3479.3 FEET PER SECOND

PIEZOMETRIC EFFICIENCY IS 47.0 PERCENT

CORRECTED PIEZOMETRIC EFFICIENCY IS 41.7 PERCENT

BALLISTIC EFFICIENCY IS 73.4 PERCENT

(The reverse of this page is blank.)

21

Figure 6. Graph of 20mm Performance 0.020 Web.

TABLE IV. INTERIOR BALLISTIC PROGRAM FORTRAN 4 LISTING.

```
PROGRAM PDGSX(INPUT,OUTPUT,TAPE5=INPUT,TAPE6=OUTPUT,FILMPL)    P095800   00001
            F99 SADLER. J    1110254341 H958-2 095AG1 00109   9   P0958   00003
$0 0/0 NO PLOT                                                      P0958   00004
      CFXFCUTE      IMJOH                                          P0958   00005
      FTAJOH         MAP                                           P0958   00006
      FIHFTC 06M                                                   P0958   00007
      COMMON/   /PCPWS(1000),PWUIS(1000),WUN,PTOP,NPTS             P0958   00008
      DIMENSION PSY(20),VEE(20)                                    P0958   00009
      DIMENSION PMS(20),NATE(20),TYPE(N)                           P0958   00010
    2 FORMAT(FM,1,FR,3,FR,4,FH,2,4A2)                              P0958   00011
      WFAI(5,94)PRS                                                P0958   00012
    4 FORMAT(10FH,1)                                               P0958   00013
    6 FORMAT(5,5)NATE                                              P0958   00014
      WFAI(10FH,3)                                                 P0958   00015
   24 FORMAT(10FH,1)VEE                                            P0958   00016
      WFAI(5,26)PSY                                                P0958   00017
   26 FORMAT(10FH,3)                                               P0958   00018
      WTT=1.5                                                      P0958   00019
      TAN=GAMA/(GAMA-1.)                                           P0958   00020
    4 WFAI(5,7)AWEA,CVOL,SHOT,RUN,WEH,WETA,CHG,SCPRS               P0958   00021
    7 FORMAT(F7,3,F7,3,F7,1,F7,4,F7,2,F7,3,FA,1)                   P0958   00022
      NPTS=U                                                       P0958   00023
      MP=0.                                                        P0958   00024
      VFL=0.                                                       P0958   00025
      WAHF2.*CHG/(WWO*EB)                                          P0958   00026
      WTTF(6,M)                                                    P0958   00027
    8 FORMAT(1M1,4IM SHOT WT.   CHARGE     WEB     M.LENGTH  CMB VOL  P0958  00028
     1HOWF AWEA//)                                                 P0958   00029
      WHTF(6,9)SHOT,CHG,WEB,WUN,CVOL,AWEA                          P0958   00030
    9 FORMAT(F10.2,F10.3,F10.4,F10.1,F10.2,F10.2///)               P0958   00031
      WHTF(6,35)(TYPE(N),N=1,4)                                    P0958   00032
   35 FORMAT(32H PROPELLANT USED IN DEVICE IS  ,4A2,///)           P0958   00033
      WHTF(6,27)                                                   P0958   00034
   27 FORMAT(101H    TIME     CHAMB PRES    TRAVEL      PRO         P0958   00035
     1P BURNED    PRES SLOPE    VELOCITY    BS PRES//)             P0958   00036
      MP=0.0                                                       P0958   00037
      VEI=U.                                                       P0958   00038
                                                                   P0958   00039
                                                                   P0958   00040
```

24

```
        MDTS=0.0
        PTOP=3000.
        CPRS=SCPMS
        GAMH=(1.+HETA)*(GAMA-1.)
        DO 30 J=1,750.1
   74   JA=1
   78   IF(CPMS-PMS(JA))77,76,75
   75   JA=JA+1
   76   H=RATE(JA)
        GO TO 7H
   74   H=RATE(JA)
        GO TO 10
   77   DIT=PMS(JA)-PMS(JA-1)
        DAT=RATE(JA)-RATE(JA-1)
        PIG=CPRS-PMS(JA-))
        OIM=((P)G/DIT)*DAT)
        H=RATE(JA-1)+OIM
   10   IF (HP-CHG)11,80,80
   80   DNDT=0
        GO TO 12
   11   DNDT=M*HMO*HAHE
        HP=HP+(DNDT*.000025)
   12   VEL1=VFL2
        MTM=(VEL2*VEL2)/(GAMA*32.17*FI*P*PIT)
        HDOT=1./(1.+((GAMA-1.)/2.)*RTM))
        TUT=HDOT**TAD
        PHEX=CPHS*TUT
        KO=)
   50   IF(VFE(KO)-VEL2)51,52,53
   51   KO=KO+1
   52   PFAC=PSY(KO)
        GO TO 59
   53   HAG=(VEL2-VEE(KO-1))/(VEE(KO)-VEE(KO-1))
        PFAC=((PSY(KO)-PSY(KO-1))*HAG)+PSY(KO-1)
   59   FM=(SHOT+(CHG/PFAC))/32.17
        ACFL=PHEX*AREA*32.17/SHOT
        VEL2=VFL1+(ACEL*.000025)
        ACOL=(ACEL*.000025)/2.
        HINC=(VEL1*.000025)+(ACOL*.000025)
        MDTS=MDIS+(HINC*12.)
   13   AVOL=CVOL+(MDIS*AREA)
        OLDT=VFL2
        UHW=(CHG-HP)/HHO
        COVL=CVL*HP
        DPDT=((DNDT*EF*HP*12.)-((GAMH*EFM*ACEL*VEL2*12.)+(AREA*PREX*VEL1*12
       1.)))/(AVOL-(UHW*COVL))
        DOPT=J
        TIME=DOPE*.000025
        FPU=HP/CHG
        IF(CPHS.GT.PTOP) PTOP=CPHS
   15   WRITE(6,17)TIMF,CPRS,BDIS,FPU,DPDT,OLDT,PREX
```

```
      WRITE (6,17) TIMF,CPRS,BDIS,FPU,DPUT,DLDT,PREX
   15 WRITE (6,17) TIMF,CPRS,BDIS,FPU,DPUT,DLDT,PREX
   17 FORMAT(F15.4,F15.1,F15.3,F15.4,F15.1,F15.2,F10.1)
      NPTS=NPTS+1
      PCPRS(NPTS)=CPRS
      PRDIS(NPTS)=BDIS
      CPRS=CPRS+(DPUT*.000025)
      IF(BDIS.GE.RUN) GO TO 79
   39 CONTINUE
   79 DELV=VEL2-VEL1
      DRUN=BDIS-RUN
      ADV=(1.-(DRUN/(DRUNC*12.)))*DELV
      VM=VEL1+ADV
      AO=(VM*VM/RUN)*SHOT*12./(AREA*64.4)
      WRITE(6,40)AO
   40 FORMAT(//25H PIEZOMETRIC PRESSURE IS ,F9.2,//)
      WRITE(6,41)VM
   41 FORMAT(//14H MUZZLE VELOCITY IS,F4.1,16H FEET PER SECOND/)
      AK=AO/PTOP
      AF=AK*100.
      WRITE(6,42)AF
   42 FORMAT(//26H PIEZOMETRIC EFFICIENCY IS,F7.1,8H PERCENT)
      AM=(AF*EFM*32.17)/SHOT
      FKF=(VM*VM*SHOT)/(2.*32.17)
      TE=CHG*FIMP/(GAMA-1.)
      HE=FKE/TE*100.
      WRITE(6,44)AH
   44 FORMAT(//36H CORRECTED PIEZOMETRIC EFFICIENCY IS,F7.1,8H PERCENT)
      WRITE(6,43)HE
   43 FORMAT(//24H BALLISTIC EFFICIENCY IS,F8.1,8H PERCENT)
      CALL MPLOT
      GO TO 6
      END
$IBFTC MPLOT
      SUBROUTINE MPLOT
      COMMON/   /PCPRS(1000),PRDIS(1000),RUN,PTOP,NPTS
      I=0
      XL=PRDIS(1)
      XH=PRDIS(NPTS)
      YH=PCPRS(1)
      YT=PTOP
      CALL DXDYV(1,XL,AH,DX,N,I,NX,20.0,IERR)
      CALL DXDYV(2,YH,YT,DY,M,J,NY,20.0,IERR)
      IS=-I
      J=-J
      CALL GRIDV(L,XL,XR,YB,YT,DX,DY,N,M,I,J,NX,NY)
      CALL PRINTV(-4,4HRDIS,500,10)
      CALL APRNTV(0,-16,-4,4HCPRS,10,500)
      CALL APLOTV(NPTS,PT(1),PR1(1),1,1,55,IERR)
      CALL APLOTV(NPTS,PT(1),PR2(1),1,1,38,IERR)
      IX1=NAV(PRDIS(1))
      IY1=NYV(PCPRS(1))
      DO 300 IKK=2,NPTS
      IX2=NAV(PRDIS(IKK))
      IY2=NYV(PCPRS(IKK))
      CALL LINEV(IX1,IY1,IX2,IY2)
      IX1=IX2
      IY1=IY2
  300 CONTINUE
      RETURN
      END
```

(The reverse of this page is blank.)

25

SECTION IV

EXPERIMENTAL RESULTS

NORMAL DEFLAGRATION

The validity of the preceding analysis is easily assessed by measuring the pressure-time history and muzzle velocity of a given device and correlating the results with those predicted by the theory. This experimental effort was conducted at the Jet Propulsion Laboratory of the California Institute of Technology under NASA sponsorship. The device which was used for this purpose is shown in Figure 7.

Figure 7.   Device to Measure Pressure-Time History and Muzzle Velocity.

Pressures were measured in the chamber and at two additional
points down the barrel by means of high-pressure Kistler piezometric
pressure transducers feeding Kistler charge amplifiers and recorded on
persistent phosphor Techtronix oscilloscopes. Muzzle velocities were
measured by means of break screens connected to Hewlett-Packard digital
clocks.

The launch tube was of smooth bore configuration and for maximum
flexibility was constructed with a uniform bore diameter rather than
with an expanded chamber; this design allows an infinitely variable
chamber volume. Ignition and propellant loading techniques are shown
in Figure 8.
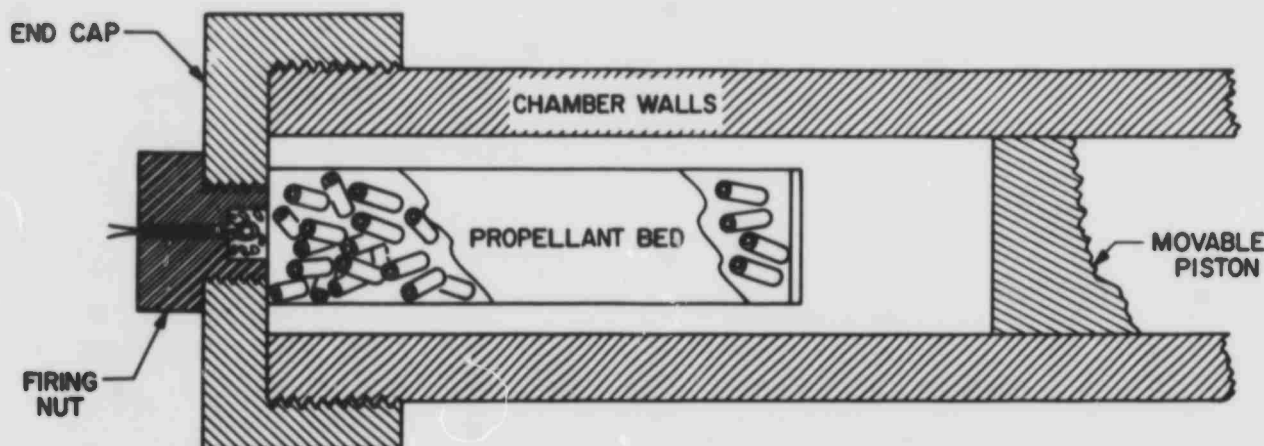
Figure 8. Ignition and Propellant Loading Techniques.

The initial chamber volume is determined by the location of the
piston base while the loading volume is a function of the diameter and
length of the phenolic sleeve into which the propellant is initially
packed. The ignitor used consists of a firing nut containing an Atlas
electric match surrounded by 300 mg of black powder. This type igniter
gives a short-duration flame of high intensity with little brisance.
When the tubular propellant grains are not too tightly packed, the
effect of the phenolic loading sleeve may be neglected except insofar
as the volume it displaces is concerned.

Firings demonstrating proper deflagration and typical correlation
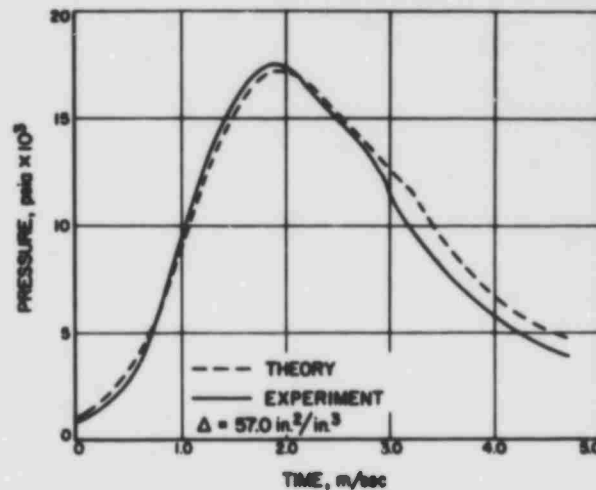with the above referenced theory are illustrated in Figures 9, 10, and

28

Figure 9. Pressure Time Plot With $\Delta = 57.0$ in.^{2}/in.^{3}.

11. A qualitative delineation of the phenomena occurring in Figure 9, for example, would be as follows:

     1. t = 0 to t = 1.0 m/sec: Very slow increase in chamber volume as the result of an almost negligible projectile velocity, hence very rapid pressure increase due to energy release by propellant in almost constant chamber volume.

     2. t = 1.0 m/sec to t = 1.9 m/sec: Projectile velocity increasing and, thus, exposed chamber volume increasing more rapidly. Excess energy input decreasing as function of incremental volume to be pressurized.

     3. Peak pressure (t = 1.9) to propellant burnout (t = 2.9 experimentally, 3.2 analytically): Plenum volume increasing more rapidly than energy input. Sharp break in curve slope due to propellant burnout.

     4. Subsequent to burnout, a very rapid pressure decrease occurs as a result of the expansion of the gases, heat loss to tube, and further energy imparted to projectile.
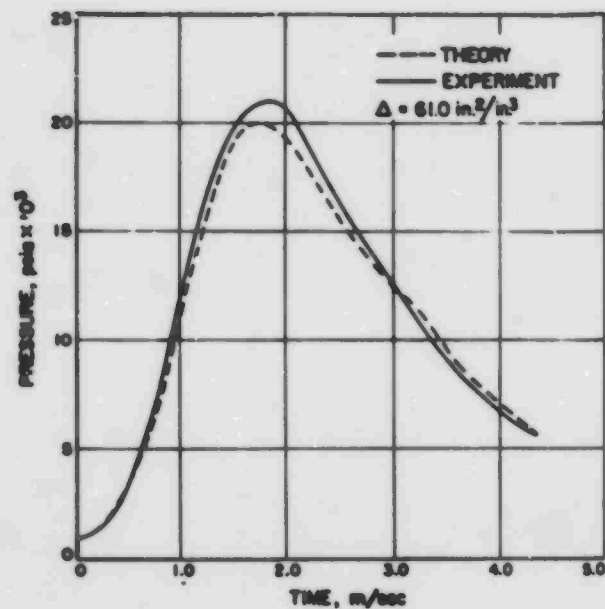
29

Figure 10. Pressure Time Plot With Δ = 61.0 in.^{2}/in.^{3}.
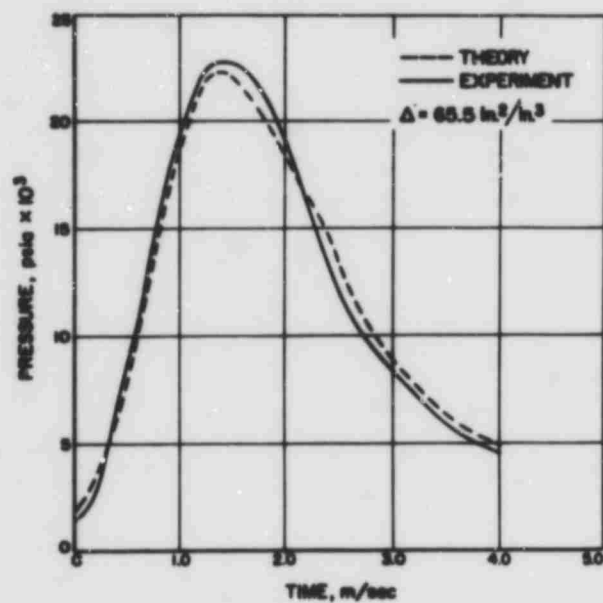

Figure 11. Pressure Time Plot With Δ = 65.5 in.^{2}/in.^{3}.

In these three firings, the primary difference exhibited between the experimental data and the analysis is a result of the following factor: the single-perforate propellant is assumed to burn externally and internally in a radial manner until the total charge is consumed.

In reality, this does not occur. A certain fraction of the grains fragment during combustion, and this increases the exposed burning surface and, in general, leads to slightly higher peak pressures and somewhat earlier web burnout than is analytically predicted. The difference, typically, is of only a few percent in peak pressure and is of such a nature that there is no way to express it analytically.

Figures 9, 10, and 11 show the quite good correlation between theory and experiment which is attainable when the density of loading Δ is kept at less than 75 in.^{2}/in.^{3}. At loadings above this level, a different mechanism of combustion becomes manifest and could probably be best described as a transition through shock-driven deflagration to virtual charge detonation. The charge characteristics are presented in Table V.

TABLE V. CHARGE CHARACTERISTICS.

Plot References	Charge Weight (gm)	Propellant Web (in.)	Slug Weight (gm)	Δ (in.^{2}/in.^{3})	Muzzle Velocity (fps)	
					Predicted	Actual
Figure 9	86.2	0.0164	560	57.0	2,080	2,040
Figure 10	90.0	0.0164	560	61.0	2,220	2,210
Figure 11	110.0	0.0190	508	65.5	2,360	2,300
Figure 12	97.5	0.0164	560	76.7	2,250	2,150
Figure 13	93.0	0.0164	550	80.0	2,190	2,220
Figure 14	105.0	0.0164	560	82.0	2,350	2,700

SHOCK-DRIVEN DEFLAGRATION

It was mentioned previously that the phenolic tube had no effect on the interior ballistic solution. This is not true, however, if the propellant is packed too tightly into the tube. The propellant used was M-10, which is virtually 100 percent nitrocellulose with no nitroglycerine

31

loading and, hence, would be expected to be relatively insensitive to detonation characteristics.

Figures 12, 13, and 14 show this phenomenon of transition from weak shock-driven deflagration to strongly shock-driven deflagration. Figure 15 shows the remains of an end cap when loading was increased to the point where a response similar to complete detonation occurred. No pressure record is available for this firing because the breech pressure transducer was also destroyed. An indirect method of pressure determination may be made by the calculation of the force necessary to shear the normalized 4130 end cap and indicates a peak pressure of at least 450,000 psig.
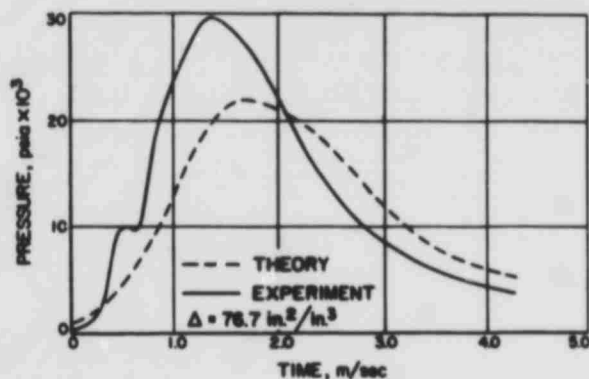
Figure 12.   Pressure Time Plot With $\Delta = 76.7$ in.^{2}/in.^{3}.

From the illustrated firings, it is possible to characterize the combustion of the propellant into various regimes as a function of the burning surface per unit of free initial volume. Symbolically, this would be

$$\Delta = S_B / V_{IF}$$

as

$$S_B = 2 \, C_w / \rho_p \, w_o$$
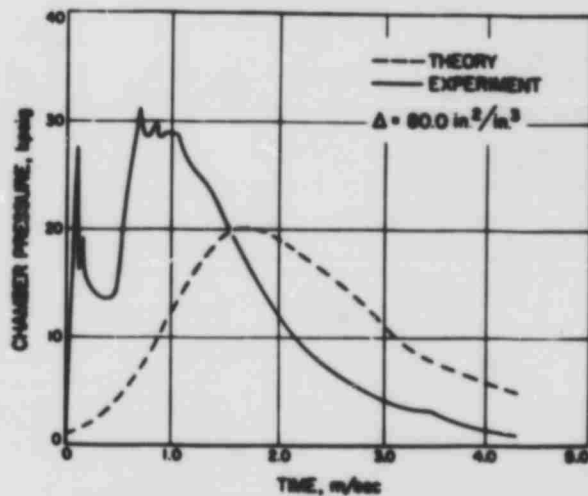
then

$$V_{IF} = L \, A_p - C_w / \rho_p$$

32

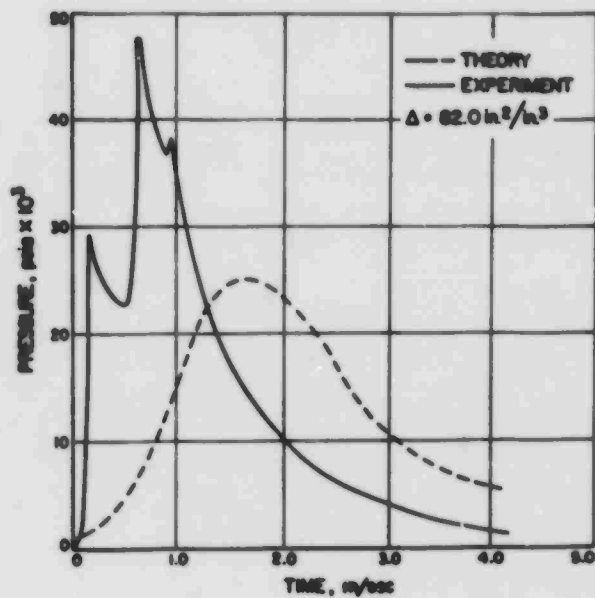Figure 13. Pressure Time Plot With Δ = 80.0 in.^{2}/in.^{3}.

Figure 14. Pressure Time Plot With Δ = 82.0 in.^{2}/in.^{3}.

It was mentioned earlier that, for proper deflagration in this system, Δ must be less than 75 in.^{2}/in.^{3}. In Figure 12, Δ = 76.7 in.^{2}/in.^{3} and it was seen that a slight pressure pulse occurs, then damps out, but drives the peak pressure to a value approximately 30 percent higher than what would have been encountered during proper deflagration.
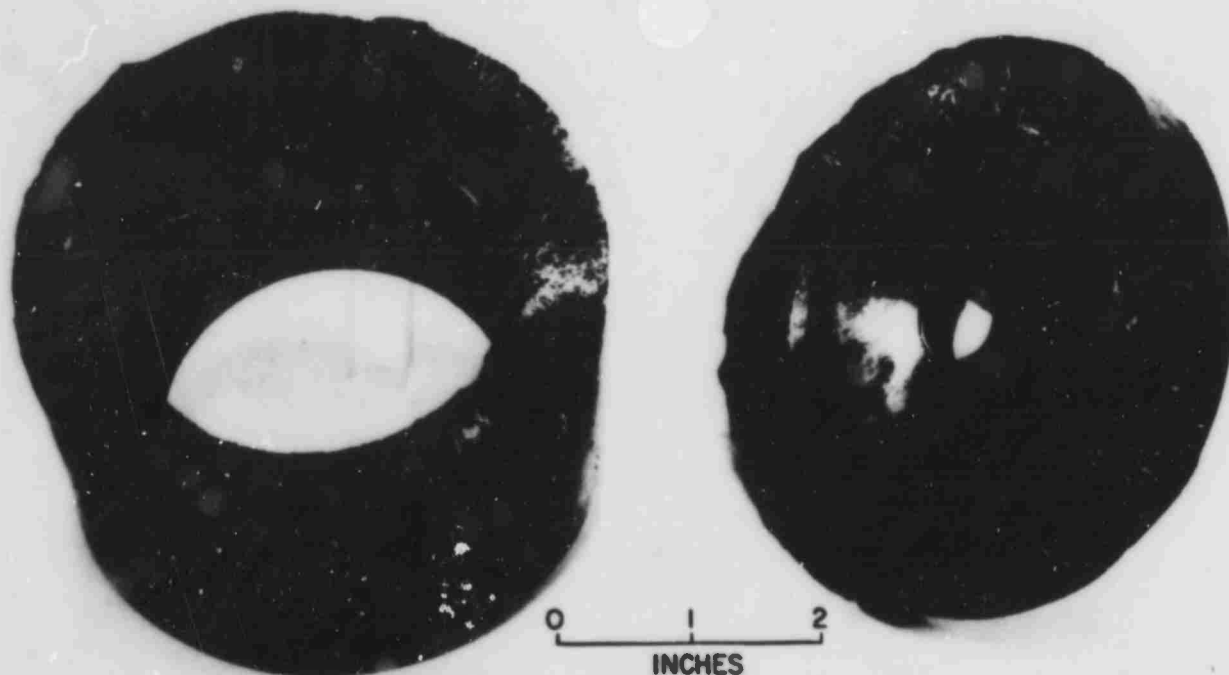
33

Figure 15. End Cap After Detonative Reaction.

In Figure 13, for which Δ = 80 in.^{2}/in.^{3}, the initial pressure spike is rapid and narrow and quickly decays to be followed by another broader pressure pulse to approximately the same value. Figure 14 shows the pressure-time profile of a loading with a Δ = 82 in.^{2}/in.^{3}.

The initial pressure wave is virtually identical to that exhibited by the previous loading. The second spike, however, is much higher and gives a peak pressure almost 100 percent higher than would be expected if linear regression were the only mechanism at work.

The loading represented by the wreckage shown in Figure 15 was Δ = 86.5 in.^{2}/in.^{3}. A detonation-like reaction phenomenon had occurred, resulting in a pressure probably well above the 450,000 psig mentioned previously. The response could have been a true detonation of the individual propellant grains, which then formed a gaseous blast over-pressure wave to act on the restraining steel. The energy release rate was such that this is the most likely mode of reaction.

34

The Δ values given for the onset of this highly undesirable mode of reaction would include most fully loaded cartridge cases with thin web propellant. This demonstrates the requirements for either deterring or inhibiting a large fraction of the initial surface area. Good ballistic design, however, requires a tradeoff between reproducible ignition and the formation of these dangerous shock waves in the deflagrating propellant bed.

From the previous results for the system under consideration, the following regimes can be defined:

$$\Delta < 75 \qquad \text{Proper deflagration}$$
$$75 < \Delta < 86 \qquad \text{Shock-driven deflagration}$$
$$\Delta > 86 \qquad \text{Detonation like response}$$

These particular Δ values are doubtless a function of propellant composition and ignition technique. They do graphically demonstrate, however, that the ballistic designer must be cautious when approaching very high loading densities to be certain that the regimes, other than normal propellant regression, are avoided.

REFERENCES

1. Heiney, O.K., "Simplified Interior Ballistics of Propellant Actuated Devices," JPL SPS 47-43.

2. Corner, J., "Theory of the Interior Ballistics of Guns," John Wiley, New York, 1950.

3. Hirschfelder, Kershner, and Curtiss, "Interior Ballistics," Volumes I and II, February and April 1943, NDRC Reports A-142 and A-180 (declassified).

4. Kent, R. H., "Some Special Solutions for the Motion of the Powder Gas," Physics 7, 1936.

5. NACA Report 1135, "Equations, Tables and Charts for Compressible Flow," 1953.

6. Serebryakov, M.E., "Interior Ballistics," Moscow 1949, translated at Catholic University of America under Contract NORD 10, 260

7. CPIA, "Solid Propellant Manual," Chamical Propulsion Information Agency, Johns Hopkins University, Silver Spring, Md, 1965 (Confidential).

8. "Internal Ballistics," Philosophical Library, New York, 1951.

9. "Interior Ballistics of Guns," U. S. Army Materiel Command Pamphlet 706-150, February 1965.

10. Heiney, O.K., "A New Computer-Oriented Formulism for Gun Ballistics," Volume II, 3rd ICRPG/AIAA Solid Propulsion Conference Proceedings, CPIA Publication, April 1968.

DOCUMENT CONTROL DATA - R & D

(Security classification of title, body of abstract and indexing annotation must be entered when the overall report is classified)

1 ORIGINATING ACTIVITY (Corporate author)	2a. REPORT SECURITY CLASSIFICATION
Air Force Armament Laboratory Air Force Systems Command Eglin Air Force Base, Florida	UNCLASSIFIED
	2b. GROUP

3 REPORT TITLE

ANALYTIC AND EXPERIMENTAL INTERIOR BALLISTICS OF CLOSED BREECH GUNS

4 DESCRIPTIVE NOTES (Type of report and inclusive dates)

Final Report

5 AUTHOR(S) (First name, middle initial, last name)

Heiney, Otto K., 1st Lt, USAFR

6 REPORT DATE	7a. TOTAL NO. OF PAGES	7b. NO. OF REFS
May 1969	46	10

8a CONTRACT OR GRANT NO.	9a. ORIGINATOR'S REPORT NUMBER(S)
b. PROJECT NO 62405094-2560	AFATL-TR-69-42
c.	9b. OTHER REPORT NO(S) (Any other numbers that may be assigned this report)
d.	

10. DISTRIBUTION STATEMENT This document is subject to special export controls, and each transmittal to foreign nationals or foreign governments may be made only with prior approval of the Air Force Armament Laboratory (ATWG), Eglin Air Force Base, Florida 32542.

11. SUPPLEMENTARY NOTES	12. SPONSORING MILITARY ACTIVITY
Available in DDC	Air Force Systems Command Andrews AFB, Wash, DC 20331

13. ABSTRACT

A closed breech incremental interior ballistic formulism is presented along with a Fortran 4 computer program which utilizes the system. Typical input and output data, both plotted and tabular, are included. A unique characteristic of the system is that it avoids the inaccuracies associated with approximate analytic propellant regression expressions in that regression rates are determined by a tabular routine. Various pressure gradient expressions are investigated. Correlation of the mathematical model and computer predictions to experimental device firings are presented. A shock-driven deflagration effect which may be initiated during the ignition transient is described and a postulated correlation parameter defined.

DD FORM 1473
1 NOV 68

Interior ballistics
Ammunition propellants
Guns